An Optimal Control Problem for a Rotating Elastic Crane-Trolley-Load System

Sven-Joachim Kimmerle *,** **Matthias Gerdts** *,*** **Roland Herzog** ****

* *University of the German Federal Armed Forces Munich, Institute of Mathematics and Computer Applications (LRT-1), 85577 Neubiberg/München, Werner-Heisenberg-Weg 39, Germany*
** *(e-mail: sven-joachim.kimmerle@unibw.de)*
*** *(e-mail: matthias.gerdts@unibw.de)*
**** *Technical University Chemnitz, Faculty of Mathematics, Reichenhainer Str. 41, 09107 Chemnitz, Germany*
(e-mail: roland.herzog@mathematik.tu-chemnitz.de)

Abstract: In this study we present an extension of a model of an elastic crane transporting a load by means of controlling the crane trolley motion and the crane rotation. In addition to the model considered in Kimmerle et al. (2017), we allow for rotations of the crane and include damping of the trolley and moments of inertia as well.
We derive a fully coupled system of ordinary differential equations (ODE), representing the trolley and load (modelled as a pendulum), and partial differential equations (PDE), i.e. the linear elasticity equations for the deformed crane beam. The objective to be minimized is a linear combination of the terminal time, the control effort, the kinetic energy of the load, and penalty terms for the terminal conditions.
We show the Fréchet-differentiability of the mechanical displacement field with respect to the location of the boundary condition that is moving. This is a crucial point for a further analysis on the existence of optimal controls and the derivation of necessary optimality conditions. Finally we present first results for the full time-optimal control of the extended model.

Keywords: Time-optimal control, coupling models, coupled ODE-PDE system, partial differential equations, ordinary differential equations, numeric control, numerical simulation, crane-trolley-load system, ODE-PDE constrained optimization, Fréchet-differentiability

1. INTRODUCTION

The optimal control problem for a trolley-load system without elastic deformations has been examined by Chen and Gerdts (see Chen et al. (2012) and the references therein). For the need and the challenges of the control of a real crane system see, e.g., Aschemann (2009) in the context of large overhead cranes. The optimal control of an elastic crane-trolley-system without (i) rotations around the vertical axis, (ii) damping of the trolley, and (iii) moments of inertia has been considered in Kimmerle et al. (2017). In the latter paper the problem is derived for the special case, where the pendulum modelling a load is restricted to the 2D plane; the well-posedness of the coupled ODE-PDE system is demonstrated; and results for numerical optimal control for a fixed terminal time are presented. For an overview on other coupled ODE-PDE systems, their relevance, and their optimal control, we refer also to the mentioned study.

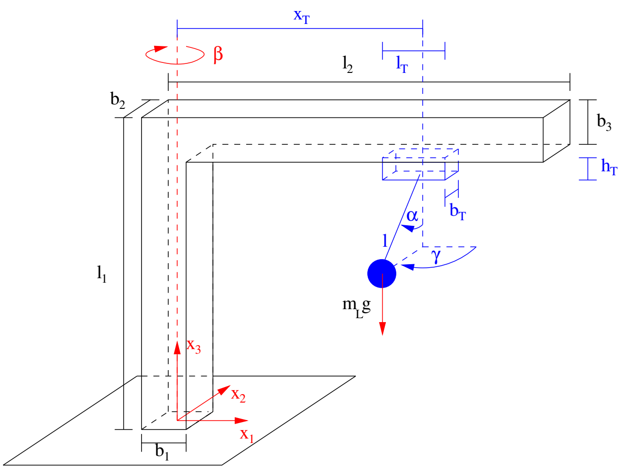

Fig. 1. Configuration of the elastic crane (within Lagrangian coordinates).

2. MODEL OF A ROTATING ELASTIC CRANE

2.1 Geometry

At first we consider a crane without any deformation and any rotation, i.e. $\beta = 0$, see Fig. 1. The domain $\Omega := \{\underline{x} := [x_1, x_2, x_3] \in \mathbb{R}^3 \,|\, b_1/2 \le x_1 \le \ell_2 - b_1/2, |x_2| \le b_2/2, \ell_1 - b_3 \le x_3 \le \ell_1\}$ prescribes the undeformed extension arm of the crane. On $\Gamma_D := \partial\Omega \cap \{\underline{x} \in \mathbb{R}^3 \,|\, x_1 = b_1/2\}$ the extension arm is fixed, yielding a homogeneous Dirichlet boundary condition (b.c) for the mechanical displacement field. The remaining boundary $\Gamma_N := \partial\Omega \setminus \overline{\Gamma_D}$ is subject to Neumann b.c. prescribing traction by area forces. The time interval $[0,T] \subset \mathbb{R}$ is assumed to be nonempty and compact, furthermore $T > 0$.

The trolley may be moved on rails, modelled by translating the x_1-position $x_T(t)$ of its center of mass. In good approximation we consider here a flat trolley with $h_T = 0$. Let $\underline{e}_i$, $i = 1, 2, 3$, denote the unit vectors. On the contact boundary $\Gamma_T(x_T(t)) := \{x \in \Gamma_N \,|\, |x_1 - x_T(t)| \le \ell_T/2, |x_2| \le b_T/2, x_3 = \ell_1 - b_3\} = x_T(t)\,\underline{e}_1 + \Gamma_T(x_T(0))$ varying with time, a force is exerted by the trolley on the extension arm. By a load, a force is applied on the trolley at its center of mass, located at $\underline{r_M}(t) := [x_T(t), 0, \ell_1 - b_3]^\top$ in the undeformed beam. This load is modelled as a pendulum of length ℓ with mass m_L.

Application of a force U_1 at the trolley's center of gravity allows to control the trolley. Application of a torsional moment U_2 around the x_3-axis at the bearing of the crane beam allows to rotate the crane by an angle β. We impose the state constraints

$$(b_1 + \ell_T)/2 \le x_T \le \ell_2 - (b_1 + \ell_T)/2, \tag{1}$$

modelling that the trolley is fixed to rails (on the crane beam with a finite extension), and

$$|\alpha| \le \mathit{const} < \pi/2 \tag{2}$$

for some constant, since the load is connected by a massless cable (and not by a rigid rod) to the trolley.

2.2 Strains and Stresses in a Beam

Within the domain of the crane we wish to solve for the mechanical displacement field $\underline{u}$. For a realistic crane we may assume small displacement gradients and, hence, model the elastic deformations of the crane beam in linear elasticity. In the approximation of linear elasticity the representation of strains and stresses within the reference (undeformed) configuration $\Omega \subset \mathbb{R}^3$ (in Lagrangian coordinates $\underline{x}$) and the current (deformed) configuration $\hat{\Omega} \subset \mathbb{R}^3$ (in Eulerian coordinates $\hat{\underline{x}}$) coincide. We assume a bijective smooth mapping between the coordinates of both descriptions. Without loss of generality (w.l.o.g.) we work in the reference configuration whenever it makes a difference. As reference configuration we consider the crane that is without any strains or stresses. The deformation depends by means of the control on time. Thus the mechanical displacement field reads $\underline{u} : \Omega \times [0,T] \to \hat{\Omega}$, $(\underline{x}, t) \mapsto \underline{u}(\underline{x}, t) = \hat{\underline{x}}(\underline{x}, t) - \underline{x}$, where we do not consider rigid body rotations or translations for the moment. The symmetrized strain is $\epsilon(\underline{u}) := (\nabla\underline{u} + \nabla\underline{u}^\top)/2$ and as a constitutive assumption we work with the Cauchy stress tensor $\sigma(\underline{u}) := \lambda \mathrm{tr}(\epsilon(\underline{u}))\mathbf{1} + 2\mu\epsilon(\underline{u})$, where $\lambda, \mu > 0$ are the Lamé constants that are related to the Young modulus E and the Poisson ratio ν of the material. tr denotes the trace of a matrix and $\mathbf{1}$ is the unity matrix. We make the assumption that the crane has a constant density $\rho > 0$.

2.3 Governing Equations for the Crane

In this subsection we derive the equations of motion for the trolley, the load, and for the deformed crane.

ODE for the Trolley-Load System. In this subsection we formulate all equations and quantities within the reference configuration. From here on we include clockwise rotations of the crane by β into our considerations. The corresponding rotation matrix w.r.t. the x_3-axis is

$$S_3(\beta) := \begin{bmatrix} \cos\beta & -\sin\beta & 0 \\ \sin\beta & \cos\beta & 0 \\ 0 & 0 & 1 \end{bmatrix}$$

and has the inverse $S_3^{-1}(\beta) = S_3(-\beta)$. Consequently, we consider then as reference configuration (from here on depending on t)

$$\Omega(t) := S_3(\beta(t))\Omega = \{\underline{x} \in \mathbb{R}^3 \,|\, S_3^{-1}(\beta(t))\underline{x} \in \Omega\}$$

and redefine analogously $\partial\Omega(t), \Gamma_D(t), \Gamma_N(t), \Gamma_T(t, x_T(t))$ by incorporating β. We assume that we may neglect the deformation of the trolley, since $h_T = 0 \ll b_3$, and of the cable between trolley and load.

The trolley's center of gravity at time t is given by

$$\underline{r_T}(t) := S_3(\beta(t))\left(\underline{r_M}(t) + \underline{u}(\underline{r_M}(t), t)\right), \tag{3}$$

the load's center of gravity at time t is given by

$$\underline{r_L}(t) := \underline{r_T}(t) - S_3(\beta(t))S_3(\gamma(t))S_2(\alpha(t))\,\ell\,\underline{e_3}$$

with the rotation matrix

$$S_2(\alpha) := \begin{bmatrix} \cos\alpha & 0 & -\sin\alpha \\ 0 & 1 & 0 \\ \sin\alpha & 0 & \cos\alpha \end{bmatrix},$$

where α is positive for a counterclockwise rotation around the x_2-axis. Since $S_3(\beta)S_3(\gamma) = S_3(\beta + \gamma)$ holds, we substitute $\tilde{\gamma} := \beta + \gamma$, $\tilde{\gamma}$ being positive for a clockwise rotation around the x_3-axis.

Let $\underline{\omega_T} := [0, 0, \dot{\beta}, 0]^\top$ and $\underline{\omega_L} := [0, \dot{\alpha}, \dot{\beta}, \dot{\tilde{\gamma}}]^\top$ be the vectors of generalized angular velocities of the trolley and the load. The kinetic energy of the mechanical system with the generalized coordinates $\underline{q} = [x_T, \alpha, \beta, \tilde{\gamma}]^\top$ is given by

$$\mathcal{T}(\underline{q}, \underline{\dot{q}}, \underline{u}) = \frac{1}{2}\left(m_T\|\dot{r}_T\|^2 + m_L\|\dot{r}_L\|^2\right) + \frac{1}{2}\left(\underline{\omega_T}^\top J_T \underline{\omega_T} + \underline{\omega_L}^\top J_L \underline{\omega_L}\right), \tag{4}$$

where m_T and m_L denote the masses of the trolley and the load and the diagonal matrices $J_T = [J_{T,\alpha}, J_{T,\beta}, J_{T,\tilde{\gamma}}]$ and $J_L = [J_{L,\alpha}, J_{L,\beta}, J_{L,\tilde{\gamma}}]$ denote the principal moments of inertia of trolley and load, respectively. Since the trolley is fixed to rails $J_{T,\alpha} = 0$ and since it is assumed to be flat, i.e. $h_T = 0$, we may neglect $J_{T,\tilde{\beta}}$ and $J_{T,\tilde{\gamma}}$ as well.

The vector of the external generalized forces, i.e. the control acting along the (deformed) rail of the trolley, the gravitation, and the control moment rotating the crane around the z-axis, is

$$\underline{f_E}(\underline{q}, \underline{U}) := [U_1, -\ell m_L g \sin\alpha, U_2, 0]^\top. \tag{5}$$

Thus the generalized potential $\mathcal{V}$, fulfilling $\underline{f_E} = -\nabla\mathcal{V}$, is

$$\mathcal{V}(\underline{q}, \underline{U}) = -U_1 x_T - \ell m_L g \cos\alpha - U_2\beta,$$

uniquely determined up to a constant.

From the Euler-Lagrange equation the equations of motion follow as

$$M(\underline{q}, \underline{u})\,\underline{\ddot{q}} = \left(\underline{f_C}(\underline{q}, \underline{\dot{q}}, \underline{u}) + \underline{f_E}(\underline{q}, \underline{U}) - K\underline{\dot{q}}\right), \tag{6}$$

where $M(\underline{q}, \underline{u}) := \nabla^2_{\underline{\dot{q}},\underline{\dot{q}}}\mathcal{T}(\underline{q}, \underline{\dot{q}}, \underline{u})$ denotes the symmetric and positive semi-definite mass matrix and $\underline{f_C}(\underline{q}, \underline{\dot{q}}, \underline{u}) := \nabla_{\underline{q}}\mathcal{T}(\underline{q}, \underline{\dot{q}}, \underline{u}) - \nabla^2_{\underline{\dot{q}},\underline{q}}\mathcal{T}(\underline{q}, \underline{\dot{q}}, \underline{u})\,\underline{\dot{q}}$ denotes the generalized Coriolis forces. The diagonal matrix $K := m_L\ell\,[\kappa_T, \kappa_L, \kappa_L, \kappa_L]$

represents the (specific) damping coefficient for the trolley and the pendulum, respectively. For the derivation of the equations of motion with further details, but for the special case $\beta = \tilde{\gamma} = 0$ and $J_L = \mathbf{0}$ ($\mathbf{0}$ being the null matrix), see Kimmerle et al. (2017), .

For brevity, we abbreviate $m := (m_T + m_L)/(m_L\ell)$. Furthermore, we introduce the differential operators $D_1 u_i := \partial^2_{1,1} u_i + \partial^2_{2,1} u_i + \partial^2_{3,1} u_i$, $i = 1, 2, 3$, where we write $\partial_i := \partial_{x_i}$ for the partial derivative w.r.t. x_i. We abbreviate $\tilde{J}_L := J_L/(m_L\ell)$. Within our approximation of small displacement gradients we find for the symmetric mass matrix

$$M = m_L\ell \begin{bmatrix} m(1+2\partial_1 u_1) & M_{12} & M_{13} & M_{14} \\ \dots & \ell + \tilde{J}_{L,\alpha} & M_{23} & 0 \\ \dots & \dots & M_{33} & M_{34} \\ \dots & \dots & \dots & \ell \sin^2\alpha + \tilde{J}_{L,\beta} \end{bmatrix}$$

with $M_{12} := ((1+\partial_1 u_1)\cos\gamma + \partial_1 u_2 \sin\gamma)\cos\alpha + \partial_1 u_3 \sin\alpha$, $M_{13} := m\left((x_T + u_1)\partial_1 u_2 - (1+\partial_1 u_1)u_2\right)$, $M_{14} := (-(1+\partial_1 u_1)\sin\gamma + \partial_1 u_2 \cos\gamma)\sin\alpha$, $M_{23} := ((x_T + u_1)\sin\gamma - u_2\cos\gamma)\cos\alpha$, $M_{33} := m((x_T+u_1)^2 + u_2^2) + \tilde{J}_{L,\beta}$, and $M_{34} := ((x_T + u_1)\cos\gamma + u_2 \sin\gamma)\sin\alpha$, where we write again $\gamma = \tilde{\gamma} - \beta$ for brevity. Furthermore we have

$$\underline{f_C}(\underline{q}, \underline{\dot{q}}, \underline{u}) =$$
$$\begin{bmatrix} -m(D_1 u_1 |\dot{x}_T|^2 - ((x_T + u_1)(1 + \partial_1 u_1) + u_2 \partial_1 u_2) \\ \quad \times|\dot{\beta}|^2) + (((1+\partial_1 u_1)\cos\gamma + \partial_1 u_2 \sin\gamma)\sin\alpha \\ \quad -\partial_1 u_3 \cos\alpha)|\dot{\alpha}|^2 \\ \quad +((1+\partial_1 u_1)\cos\gamma + \partial_1 u_2 \sin\gamma)\sin\alpha\,|\dot{\tilde{\gamma}}|^2 \\ \quad +2((1+\partial_1 u_1)\sin\gamma - \partial_1 u_2\cos\gamma)\cos\alpha\,\dot{\alpha}\dot{\tilde{\gamma}}, \\ -((D_1 u_1 \cos\gamma + D_1 u_2 \sin\gamma)\cos\alpha + D_1 u_3 \sin\alpha)|\dot{x}_T|^2 \\ \quad +((x_T + u_1)\cos\gamma + u_2\sin\gamma)\cos\alpha\,|\dot{\beta}|^2 \\ \quad +\ell\sin\alpha\,\cos\alpha\,|\dot{\tilde{\gamma}}|^2 \\ \quad -2((1+\partial_1 u_1)\sin\gamma - \partial_1 u_2 \cos\gamma)\cos\alpha\,\dot{x}_T\dot{\beta}, \\ -m\left((x_T+u_1)D_1 u_2 - D_1 u_1 u_2\right)|\dot{x}_T|^2 \\ \quad ((x_T+u_1)\sin\gamma - u_2\cos\gamma)\sin\alpha\,|\dot{\alpha}|^2 \\ \quad ((x_T+u_1)\sin\gamma - u_2\cos\gamma)\sin\alpha\,|\dot{\tilde{\gamma}}|^2 \\ \quad -2m((x_T+u_1)(1+\partial_1 u_1) + u_2\partial_1 u_2)\,\dot{x}_T\dot{\beta} \\ \quad -2((x_T+u_1)\cos\gamma + u_2\sin\gamma)\cos\alpha\,\dot{\alpha}\dot{\tilde{\gamma}}, \\ \sin\alpha\left((D_1 u_1 \sin\gamma - D_1 u_2 \cos\gamma)|\dot{x}_T|^2\right. \\ \quad -((x_T+u_1)\sin\gamma - u_2\cos\gamma)|\dot{\beta}|^2 - 2((1+\partial_1 u_1) \\ \quad \times\cos\gamma + \partial_1 u_2 \sin\gamma)\,\dot{x}_T\dot{\beta} - 2\ell\cos\alpha\,\dot{\alpha}\dot{\tilde{\gamma}}) \end{bmatrix}.$$

PDE for the Elastic Crane Beam. Let $\underline{n}$ denote the outer normal to Ω. For the domain of the crane we have the following elastodynamical problem

$$\rho\,\partial_{tt}\underline{u} - \operatorname{div}\sigma(\underline{u}) = \underline{h} \qquad \text{in } \Omega\times(0,T), \tag{7}$$
$$\underline{u} = \underline{0} \qquad \text{in } \Omega\times\{t=0\}, \tag{8}$$
$$\partial_t\underline{u} = \underline{0} \qquad \text{in } \Omega\times\{t=0\}, \tag{9}$$
$$\underline{u} = \underline{0} \qquad \text{on } \Gamma_D\times(0,T), \tag{10}$$
$$-\sigma(\underline{u}).\underline{n} - \underline{g} = \underline{0} \qquad \text{on } \Gamma_N\times(0,T) \tag{11}$$

where $\underline{g} : \Gamma_N \times [0,T] \to \mathbb{R}^3$ is a boundary force (in $\mathrm{N/m^2}$). Note that friction of elastic waves might be caused e.g. by cracks in the material, electromagnetic effects or by porosity of the media. However, a friction term, proportional to $\partial_t u$, that could enter in (7), may be neglected in our situation. The term $\underline{h} := -\rho\, g\, \underline{e}_3$ in (7) models the gravity of the dead load of the crane arm.

According to (5), the gravitational force exerted by the load alone (by means of the trolley) plus the control forces (exerted by the trolley, too) acting on the deformed beam reads

$$\underline{f_E^{(C)}}(t) = \begin{bmatrix} U_1 + m_L g \sin\alpha\cos\gamma \\ U_2/x_T(t) - m_L g\sin\alpha\sin\gamma \\ -m_L g\cos\alpha \end{bmatrix}$$

expressed in Cartesian coordinates (where β does not appear since the reference configuration rotates with β). In order to transform a surface element from the reference to the deformed configuration we use Nanson's relation. Let $F_D = \mathbf{1} + \nabla\underline{u}$ be the deformation gradient, thus in the approximation of small displacement gradients

$$\det(F_D^{-1})F_D^\top \approx (1 - \operatorname{tr}(\nabla\underline{u}(\underline{x},t)))\mathbf{1} + \nabla\underline{u}(\underline{x},t)^\top.$$

In our situation $\underline{g_0} : \Gamma_N \times [0,T] \to \mathbb{R}^3$,

$$\begin{aligned} \underline{g_0}(\underline{x},t) &:= ((1 - \operatorname{tr}(\nabla\underline{u}(\underline{x},t)))\mathbf{1} + \nabla\underline{u}(\underline{x},t)^\top)\times \\ &\times [U_1(t) + m_L g\sin\alpha(t)\cos\gamma(t), U_2(t)/x_T(t) \\ &\quad - m_L g \sin\alpha(t)\sin\gamma(t), -m_L g\cos\alpha(t) - m_T g]^\top \end{aligned}$$

models the force of the trolley onto the crane by means of the boundary pressure

$$\underline{g}(\underline{x},t) := \begin{cases} \underline{g_0}(\underline{x},t)/|\Gamma_T(\cdot)| & \text{for } \underline{x}\in\Gamma_T(x_T), \\ \underline{0} & \text{for otherwise.} \end{cases}$$

We may decompose the elastodynamical PDE (7) – (11) into an equation for the longitudinal effects, $\operatorname{div}\underline{u}$, that yields the acoustic wave equation, and an equation for the transversal part, $\operatorname{rot}\underline{u}$ (yielding the so-called shear wave equation), respectively. By a dimensionalization analysis, it turns out that the speed of longitudinal acoustic waves (speed of sound) is given by $((\lambda+2\mu)/\rho)^{1/2} \approx 6.11\,\mathrm{km/s}$, whereas the speed of transversal waves is $(\mu/\rho)^{1/2} \approx 3.35\,\mathrm{km/s}$, using the values for steel. For a grid-like structure of the crane the speed of elastic waves might be even higher, hence the time derivatives in (7) may be safely neglected in a first approximation. Consistently, we may neglect terms like $\partial_t\underline{u}$ as we do in (4) as well. Thus we consider the quasi-static situation. The corresponding elastostatic problem, where time enters as a parameter, reads

$$-\operatorname{div}\sigma(\underline{u}) = \underline{h} \qquad \text{in } \Omega\times(0,T), \tag{12}$$
$$\underline{u} = \underline{0} \qquad \text{on } \Gamma_D\times(0,T), \tag{13}$$
$$-\sigma(\underline{u}).\underline{n} - \underline{g} = \underline{0} \qquad \text{on } \Gamma_N\times(0,T). \tag{14}$$

This elliptic PDE for $\underline{u}$ depends on $\underline{q}$ by means of $\underline{g}$ and $\underline{g_0}$, respectively, whereas the ODE system for $\underline{q}$ depends on first and second derivatives of $\underline{u}$. Since the coupling effect, that is not negligible in our model, takes place on Γ_T, that has a small surface area $|\Gamma_T|$, we introduce the mean values

$$\bar{\underline{u}}(t) := \frac{1}{|\Gamma_T|}\int_{\Gamma_T(x_T(t))} \underline{\tilde{D}u}(\underline{x},t)\,dx, \tag{15}$$

in the coupling terms, where we average over each component of $\underline{\tilde{D}u} := [\partial_1 u_1, \partial_1 u_2, \partial_1 u_3, D_1 u_1, D_1 u_2, D_1 u_3, \partial_1 u_2, \partial_2 u_2, \partial_3 u_3, \partial_3 u_1, \partial_3 u_2, \partial_3 u_3]^\top$. Otherwise, a PDE problem for the trolley with a point force would have to be solved. We will consider $\bar{\underline{u}}$ as an independent state variable in the following. Consequently, we modify the b.c. (14) by replacing $\underline{g}$ by a version with mean values of $\partial_i u_j$ over Γ_T.

2.4 Optimal Control Problem

We would like to transport a load at rest from an initial position x_T^0 to a terminal position x_T^f, where the load should be at rest at the terminal time T, i.e.

$$\underline{\eta}(\underline{q}(T), \underline{\dot{q}}(T)) = \underline{0}, \tag{16}$$

where we write $\underline{\eta}(\underline{q}(T), \underline{\dot{q}}(T)) := [x_T(T) - x_T^f, \alpha(T), \beta(T), \tilde{\gamma}(T), \dot{x}_T(T), \dot{\alpha}(T), \dot{\beta}(T), \dot{\tilde{\gamma}}(T)]^\top$. We would like to achieve this in minimal time T, while minimizing the swinging of the load, i.e. its kinetic energy.

The standard part of the objective, consists of a linear combination of the terminal time, a kinetic energy term, and the control efforts (acting as regularization as well)

$$\mathcal{J}_1(\underline{q}, \underline{U}, T) := \lambda_1 T + \frac{\lambda_2}{2}\left(\|\dot{\alpha}\|^2_{L^2(0,T)} + \|\dot{\tilde{\gamma}} \sin\alpha\|^2_{L^2(0,T)}\right) + \frac{\lambda_3}{2}\|U_1\|^2_{L^2(0,T)} + \frac{\lambda_4}{2}\|U_2\|^2_{L^2(0,T)}$$

with the weights $\lambda_j \geq 0$, $j = 1, \ldots, 4$, where at least one weight is strictly positive. We add terms penalizing the violation of terminal conditions

$$\mathcal{J}_2(\underline{q}(T), \underline{\dot{q}}(T))) := \frac{1}{2}\underline{\eta}(\underline{q}(T), \underline{\dot{q}}(T))^\top \operatorname{diag}(\underline{\nu})\, \underline{\eta}(\underline{q}(T), \underline{\dot{q}}(T)) + \underline{\mu}^\top \underline{\eta}(\underline{q}(T), \underline{\dot{q}}(T))$$

with the multipliers $\nu_j \geq 0$, $\mu_j \in \mathbb{R}$, $j = 1, \ldots, 8$. By adding the linear terms with the Lagrange multipliers μ_j we achieve that $\mathcal{J}_2$ is a multiplier-penalty-function that is exact (Geiger et al., 2002, Kap. 5.4). We will compute the multipliers ν_j and μ_j by means of the multiplier-penalty-method. Our objective is the Lagrangian

$$\mathcal{J}(\underline{q}, \underline{U}, T) := \mathcal{J}_1(\underline{q}, \underline{U}, T) + \mathcal{J}_2(\underline{q}(T), \underline{\dot{q}}(T)).$$

Please note that neither $\underline{u}$ nor $\underline{\bar{u}}$ does enter explicitly into the objective. If $\lambda_1 > 0$, then we consider a time-optimal control. We perform a transformation onto a fixed time interval, mapping $t \in [0, T]$ to $\tau \in [0, 1]$, thus the domain is independent of the control (parameter) T. According to the time transformation, e.g., time derivatives have to be scaled with a factor T.

Our optimal control problem is to minimize $\mathcal{F}(\underline{U}, T) := \mathcal{J}(\underline{q}(\underline{U}, T), \underline{U}, T)$ for a $\underline{U} \in U := [W^{1,\infty}(0, T)]^2$ and $T \in [0, \infty)$ under the following constraints:

- the PDE (12) with boundary conditions (13) and (14),
- the ODE system (6) where we have employed the mean values introduced in (15) (e.g. $\bar{u}_1$ instead of $\partial_1 u_1$) in M and G, together with initial conditions, e.g., $x_T(0) = x_T^0, \dot{x}_T(0) = \alpha(0) = \dot{\alpha}(0) = \beta(0) = \dot{\beta}(0) = \tilde{\gamma}(0) = \dot{\tilde{\gamma}}(0) = 0$,
- the state equation (15) for $\underline{\bar{u}}$,
- the control constraints $U_{min,i} \leq U_i \leq U_{max,i}$, $i = 1, 2$, pointwise for all $t \in [0, T]$.

In principle, we have to require:

- the terminal conditions (16),
- the state constraints (1) for the trolley position and (2) for the angle α of the load.

However, for the moment we neglect the terminal conditions (assuming that they are sufficiently accomplished by the objective $\mathcal{J}_2$) and the state constraints (as they never get active for suitable initial controls).

3. DIFFERENTIABILITY OF THE CONTROL-TO-STATE OPERATOR

We consider an abstract problem for $\underline{u} \in \mathbb{R}^d$ of the type

$$\mathcal{A}\underline{u} = \underline{h} \quad \text{in } \Omega \tag{17}$$

with an arbitrary right hand side $\underline{h} \in L^{\tilde{q}}(\Omega; \mathbb{R}^d)$, $1 \leq \tilde{q} < \infty$, on an open bounded, simply connected Lipschitz domain $\Omega \subset \mathbb{R}^d$ with $d \geq 2$ (typically $d = 3$ in our application). Let $\mathcal{A}\underline{\phi} := -\operatorname{div}(A\nabla\underline{\phi})$ be a weakly elliptic operator in divergence form, i.e. Korn's inequality holds (coercivity) and $\mathcal{A}$ is linear, continuous, and self-adjoined, mapping an arbitrary function $\underline{\phi}$ from $W^{2,\tilde{q}}(\Omega; \mathbb{R}^d) \to L^{\tilde{q}}(\Omega; \mathbb{R}^d)$.

We are interested in the differentiability of the solution $\underline{u}$ with respect to the location of boundary conditions. More precisely, we consider the boundary conditions

$$\underline{u} = 0 \qquad \text{on } \Gamma_D, \tag{18}$$

$$-A\partial_n \underline{u} = \underline{g}(\cdot; \underline{p}) \qquad \text{on } \Gamma_N, \tag{19}$$

where ∂_n denotes the normal derivative. The boundary data has the following structure:

$$\underline{g}(\underline{x}; \underline{p}) = \begin{cases} \underline{g_0}(\underline{x} - \underline{p}) & \text{where } x \in \underline{p} + B, \\ \underline{0} & \text{elsewhere.} \end{cases} \tag{20}$$

Let us suppose that the boundary Γ_N has a flat part, i.e., a part which lies in a hyperplane. In (20), $\underline{p}$ is a point on the boundary Γ_N and $B \subset \mathbb{R}^{d-1}$ is a fixed flat shape with a smooth (relative) boundary. It is reasonable (but not necessary) to suppose that $\underline{0} \in B$. The function $\underline{g_0} : B \to \mathbb{R}^d$ is supposed to be smooth, bounded, and differentiable w.r.t. states and controls. We suppose that $\underline{p} + B$ belongs to Γ_N for all values of $\underline{p} \in \Gamma'_N$ near a nominal vector $\underline{p_0}$. The boundary part $\Gamma'_N \subset \Gamma_N$ is defined s.t. $\underline{p} + B \in \Gamma_N$ for all $\underline{p} \in \Gamma'_N$. As usual we define $H^1_D(\Omega; \mathbb{R}^d) := \{\underline{\psi} \in H^1(\Omega; \mathbb{R}^d) \,|\, \underline{\psi} = \underline{0} \text{ on } \Gamma_D\}$. We consider the operator S defined by the mapping

$$\Gamma'_N \ni \underline{p} \mapsto S(\underline{p}) := \underline{u} \in H^1_D(\Omega; \mathbb{R}^d) \tag{21}$$

and wish to show its differentiability at the point $\underline{p_0}$. S is called the control-to-state operator for problem (17)–(20), where $\underline{p}$ is the control and $\underline{u}$ the sought-after state.

3.1 Fréchet-differentiability with respect to the location of the boundary condition

In this subsection we examine the F-differentiability (Fréchet-differentiability) of the control-to-state map. We remark that our approach is related partially to Hettlich (1995).

Hypothesis 1. Geometry of the shift of the boundary condition

We consider an one-dimensional Γ'_N with box constraints, w.l.o.g. let $\underline{p} = p\,\underline{\xi}$, where $\underline{\xi} \in \mathbb{R}^d$ is a fixed direction and $p \in I_p := [p_{min}, p_{max}]$ for some values p_{min} and p_{max} (corresponding, e.g., to (1)).

For simplicity, assume B to be simply connected and convex, and that we may split $\partial B = \partial B_r \cup \partial B_f \cup \partial B_p$ into disjoint boundary parts. According to the positive direction of motion of p, the boundary part ∂B_r is on the rear side, ∂B_f on the front side, and ∂B_p is a possible part of the boundary moving parallel to $\underline{p}$. For the boundary with the wall, we assume $\partial B \cap \Gamma_D = \emptyset$.

Lemma 2. Fréchet-differentiability of S w.r.t. p

Let $\Omega \subset \mathbb{R}^d$ be an open bounded, simply connected Lipschitz domain and let Hypothesis 1 for $\underline{p}$, Γ'_N, and B hold.

For p, we consider S, analogously as defined for $\underline{p} = p\,\underline{\xi}$ in (21), for the problem (17) – (20), where $\mathcal{A}\underline{\phi} = -\mathrm{div}\,(A\nabla\underline{\phi})$ is a weakly elliptic operator in divergence form. For the data let $\underline{h} \in L^{\tilde{q}}(\Omega;\mathbb{R}^d)$, where $d \le \tilde{q} < \infty$, and $\underline{g_0} \in C^0(\overline{B};\mathbb{R}^d)$ hold.
Then the operator $S \in \mathcal{L}(I_p, C^0(\Omega;\mathbb{R}^d))$ is F-differentiable. The F-derivative $S' \in \mathcal{L}(I_p, rca(\Omega;\mathbb{R}^d))$, where $rca(\Omega;\mathbb{R}^d)$ denotes the set of regular additive measures on Ω, may be identified at p by the solution of a problem of type (17) – (20) with $\underline{h} \equiv 0$ and

$$\underline{g} = \lambda_{p,B}\underline{g_0} := \left(\delta_{p\,\underline{\xi}+\partial B_f} - \delta_{p\,\underline{\xi}+\partial B_r}\right)\underline{g_0},$$

with line measures δ_D on Ω, being one on the corresponding set D and zero elsewhere.

Proof.

Step 1) The difference equation

For the moment we fix $p = p_0$. Let $S(p)$ and $S(p+\delta p)$ denote two solutions corresponding to compact supports $B_0 := \underline{p}+B = p\,\underline{\xi}+B$ and $B_+ := (p+\delta p)\underline{\xi}+B$ of $\underline{g}$ on the Neumann boundary part. The problem for their difference $\underline{\delta u} := S(p+\delta p) - S(p)$ reads according to (17) – (20)

$$\begin{aligned} -\mathrm{div}(A\nabla\,\underline{\delta u}) &= 0 && \text{in } \Omega,\\ \underline{\delta u} &= 0 && \text{in } \Gamma_D,\\ -A\partial_n\underline{\delta u} &= \underline{\delta g}(\cdot;p,\delta p) && \text{on } \Gamma_N, \end{aligned}$$

where the Neumann boundary data $\underline{\delta g}(\underline{x};p,\delta p) := g(\underline{x};(p+\delta p)\,\underline{\xi}) - g(\underline{x};p\,\underline{\xi})$ is

$$\underline{\delta g}(\underline{x};p,\delta p\,\underline{\xi}) = \begin{cases} -\underline{g_0}(\underline{x}-p\,\underline{\xi}) & ;\ \underline{x} \in B_0 \setminus B_+,\\ \underline{g_0}(\underline{x}-(p+\delta p)\,\underline{\xi}) & ;\ \underline{x} \in B_+ \setminus B_0,\\ \underline{0} & ;\ \text{elsewhere.} \end{cases}$$

By standard techniques, involving Korn's inequality (Ω is simply connected), the Hölder inequality, the trace theorem and the Sobolev embedding, we obtain the existence of a unique solution satisfying the estimate

$$\|\underline{\delta u}\|_{W^{1,\tilde{q}}(\Omega;\mathbb{R}^d)} \le C|\delta p|\|\underline{g_0}\|_{L^\infty(B;\mathbb{R}^d)}.$$

The constant C depends on Ω, $\tilde{q}$, the space dimension d, and Korn's constant, but not on δp.

Step 2) Existence of a F-derivative

Thus $\delta S := \underline{\delta u}/|\delta p|$ is uniformly bounded in $W^{1,\tilde{q}}(\Omega;\mathbb{R}^d)$ and we may deduce from the Banach-Alaoglu theorem (Alt (2016)) the existence of a weak-$*$-convergent subsequence with a weak-$*$-limit, that we denote by $S'(\underline{p})$. Since p_0 is arbitrary, this holds for all $p \in I_p$. So far we have $S'(p) \in W^{1,\tilde{q}'}(\Omega;\mathbb{R}^d)$ with $\tilde{q}' = \tilde{q}/(\tilde{q}-1)$. By using the Sobolev embedding for $\tilde{q} \ge d$ we find $W^{1,\tilde{q}}(\Omega;\mathbb{R}^d) \hookrightarrow C^0(\Omega;\mathbb{R}^d)$ and $S' \in \mathcal{L}(I_p, rca(\Omega;\mathbb{R}^d))$ with the topological dual space $(C^0(\Omega;\mathbb{R}^d))' = rca(\Omega;\mathbb{R}^d)$ (see Alt (2016) for further details).

Step 3) Identification of the limit S'

Consider an arbitrary part $\Omega_* \subset \Omega$ for any $\underline{\psi} \in C_c^\infty(\Omega_*;\mathbb{R}^d)$ with compact support on Ω_*

$$\begin{aligned} &\int_{\Omega_*} A\nabla\delta S(p)(\underline{x}) \cdot \nabla\underline{\psi}(\underline{x})\,d\underline{x}\\ &= \frac{1}{|\delta p|}\int_{\Omega_*\cap(B_+\setminus B_0)} \underline{\delta g}(\underline{x};p,\delta p)\cdot\underline{\psi}(\underline{x})\,d\underline{x}\\ &\quad - \frac{1}{|\delta p|}\int_{\Omega_*\cap(B_0\setminus B_+)} \underline{\delta g}(\underline{x};p,\delta p)\cdot\underline{\psi}(\underline{x})\,d\underline{x}. \end{aligned}$$

Exploiting the assumptions on B, we see that for sufficiently small $|\delta p|$, δS fulfills a problem with the limit

$$\begin{aligned} -\mathrm{div}(A\nabla\,S'(p)) &= 0 && \text{in } \Omega,\\ S'(p) &= 0 && \text{in } \Gamma_D,\\ -A\partial_n S'(p) &= \lambda_{p,B}\,\underline{g_0} && \text{on } \Gamma_N, \end{aligned}$$

where $\lambda_{p,B}$ is a line measure on Ω, defined as

$$\lambda_{p,B}(x)\,\underline{g_0}(x) = \begin{cases} -\underline{g_0}(\underline{x}-\underline{p}) & \text{where } \underline{x} \in \underline{p}+\partial B_r,\\ \underline{g_0}(\underline{x}-\underline{p}) & \text{where } \underline{x} \in \underline{p}+\partial B_f,\\ \underline{0} & \text{elsewhere.} \end{cases}$$

Thus the limit problem has a unique solution S' and we have a strongly convergent sequence. □

Note that in the corresponding problem for a 1D crane beam that is not discussed in this study, the F-derivative has to be considered w.r.t. the volume force h, where the location of the support of the trolley enters and we find a limit problem with $h = \lambda_{p,B}$ and $g = 0$ (relevant only at one point at the right end of the beam).
For a proof of the well-posedness of our coupled ODE-PDE system in $d = 3$ for sufficiently small times $T > 0$, for sufficiently small contact areas $|\Gamma_T|$, and a domain $\Omega \subset \mathbb{R}^3$ with smooth corners, see Sect. 3 in Kimmerle et al. (2017), where we find for the states

$$\underline{y} := [\underline{q}, \underline{u}] \in Y := [H^2(0,T)]^2 \times L^\infty(0,T;W^{3,\tilde{p}}(\Omega;\mathbb{R}^3)),$$

for $\tilde{p} > 3$. In this case, S is F-differentiable w.r.t. U_1 and U_2, that enter linearly into the ODE and then by means of $\underline{g}$ into the PDE. Since $\underline{\bar{u}}$ appears only linearly in the ODE for $\underline{q}$, this motivates that we may expect that the (full) control-to-state operator $\tilde{S} : U \ni \underline{U} \to \underline{y} \in Y$ is F-differentiable. However, the latter has not been proved rigorously yet. Furthermore, then $\mathcal{F}$, not being explicitly dependent of u and $\underline{\bar{u}}$, is F-differentiable w.r.t. U_1 and U_2 for sufficiently small T and $|\Gamma_T|$.

4. NUMERICAL METHODS

For the numerical optimal control, we follow a first-discretize-then-optimize strategy (FDTO), since the first-optimize-then-discretize (FOTD) strategy requires the formulation of necessary optimality conditions that are not straight-forward for our coupled problem. The PDE is discretized by the finite element method and for the time-stepping scheme we use a semi-explicit method that is second-order in time. For the computation of a descent direction, sensitivity- and adjoint-based methods are, in principle, available. An adjoint-based approach might be faster in the case where the number of discretized equations is larger than the number of discretized constraints. However, due to the complicated structure of the coupled ODE-PDE model, the adjoint system has a complicated structure involving, e.g., non-standard integro-differential equations that are due to the averages $\underline{\bar{u}}$ on Γ_T. Therefore we follow a sensitivity-based FDTO approach. The descent direction is computed by a projected gradient method with a modified BFGS update for the Hessian. The BFGS method is a quasi-Newton method that may be used when the exact second-order derivatives are not available as it is here the case due to the averaging on Γ_T. We stop our

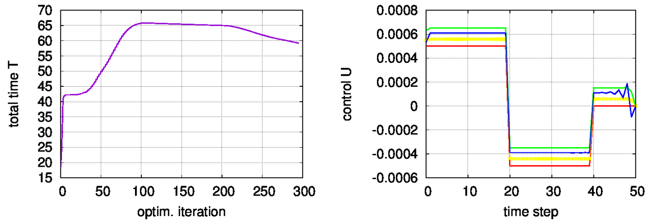

Fig. 2. Convergence of terminal T vs. inner optimization iteration (left-hand side) and optimal control U as function of the time step (right-hand side) after 0 (red), 1 (yellow), 2 (green), and 99 (blue) multiplier-penalty iterations, resp.

optimization, when the scaled updates of $\underline{U}$ and T are smaller than a certain tolerance tol_{opt}. However, for any given set of weights $\underline{\lambda}$, the feasibility could be still violated. In an outer iteration k, we take care of the violation of the terminal conditions (16) by applying a multiplier-penalty-method. We update the multipliers by

$$\mu_j^{(k)} := \mu_j^{(k)} + \nu_j^{(k)} \eta_j(\underline{q}^{(k)}(T), (\dot{\underline{q}})^{(k)}(T)),\ j = 5, \ldots, 12.$$

If a feasibility η_j has not been reduced by a certain factor $c_{M,(j)}$, $j = 1, \ldots, 8$, we multiply $\nu_j^{(k)}$ by a suitable update factor c_W. Then we restart our optimization loop, until the feasibility constraints are satisfied up to a given tolerance tol_{feas}. By this means we compute a numerical optimal control. For further details for the numerical simulation and optimal control, see Kimmerle et al. (2017).

5. NUMERICAL RESULTS

For ease of presentation and computational issues, we examine in this study only the 2D situation with $U_2 \equiv 0$ fixed (implying $\beta \equiv \gamma \equiv 0$). However, we start with an initial guess for the terminal time T far away from the solution. Here we consider $\ell = 25\,\mathrm{m}$ for the pendulum length and $E = 10^9\,\mathrm{N/m^2}$ for the unscaled Young modulus. As scaled damping coefficients we consider $\kappa_T = 10^{-3}/\mathrm{s}$ and $\kappa_L = 1\,\mathrm{m^2/s}$. When the pendulum is restricted to a plane the required principal moment of inertia is, assuming a spherical load, $J_{L,\alpha} = 2.09 \cdot 10^6\,\mathrm{kg\,m^2}$. Please note that the system with inertia, i.e. a physical pendulum with length ℓ, corresponds mathematically to a system with the so-called reduced length $\ell + \tilde{J}_{L,\alpha}$. For further technical data for the crane see Table 1 in Kimmerle et al. (2017).

In particular, we present here results for time-optimal control, see Fig. 2 for the controls and its numerical convergence, Fig. 3 for the ODE states $\underline{q}$, and Fig. 4 for the PDE state $\underline{u}$. By a further optimization of the code and using a suitable rescaling of the weights and multipliers, the computing times could be significantly decreased in comparison to the results presented in Kimmerle et al. (2017). As parameters in the algorithms we work here only with a time discretization of $T/50$ and 5400 finite elements (3D), and with the tolerances $tol_{opt} = 10^{-4}$ and $tol_{feas} = 10^{-3}$. We start with $\lambda_1 = 0.01$, $\lambda_2 = 1$, $\lambda_3 = 10^{-4}$, $\nu_1 = 1$, $\nu_2 = 0.1$, $\nu_5 = 10$, $\nu_6 = 1$, and $\underline{\mu} = \underline{0}$. We increase the multipliers, ν and μ, in the outer iteration (for updating the multiplier penalties) by a factor of $c_W = 2$. For the control constraints $U_{max} = -U_{min} = 10^{-3}\,\mathrm{s^{-2}}$ is considered, but otherwise the initial guess for U is of the same shape as in Kimmerle et al. (2017). The initial guess for T and the other parameters are chosen exactly as in the latter study.

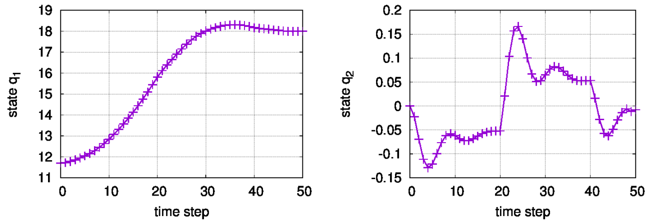

Fig. 3. ODE states vs. time step, position of trolley $q_1 = x_T$ (left-hand side) and angle of load $q_2 = \alpha$ (right-hand side).

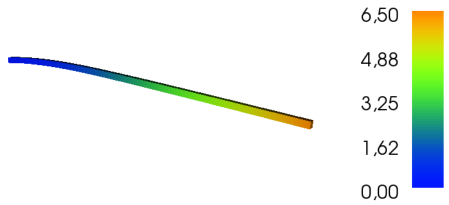

Fig. 4. Deformed crane beam at terminal time T. Colors indicate absolute mechanical displacement field $\|\underline{u}\|_2$ (m). The plotted vertical deformation of the crane beam is scaled for ease of presentation.

6. OUTLOOK

We have modelled mathematically a time-optimal control problem for a coupled ODE-PDE system, arising in applications as elastic crane-trolley-load systems. We have demonstrated the F-differentiability with respect to the location of the moving boundary condition. First numerical results for time-optimal control are presented. From a theoretical point of view, the derivation of the existence of optimal controls and the necessary optimality conditions, allowing for a FOTD approach as well, are open. A natural goal is to achieve the computation of numerical optimal control in 3D in reasonable computing times.

REFERENCES

H.W. Alt. *Linear Functional Analysis. An Application-Oriented Introduction.* Springer-Verlag, London, 2016.

H. Aschemann. Passivity-based trajectory control of an overhead crane by interconnection and damping assignment. In H. Ulbrich and L. Ginzinger, editors, *Motion and Vibration Control*, pages 21–30. Springer Science + Business Media B.V., 2009.

J. Chen and M. Gerdts. Smoothing technique of non-smooth Newton methods for control-state constrained optimal control problems. *SIAM J. Numer. Anal.*, 50: 1982–2011, 2012.

C. Geiger and C. Kanzow. *Theorie und Numerik restringierter Optimierungsaufgaben* Springer-Verlag, Berlin/Heidelberg, 2002.

F. Hettlich. Frechet derivatives in inverse obstacle scattering. *Inverse Problems*, 11:371 – 383, 1995.

S.-J. Kimmerle, M. Gerdts, and R. Herzog. Optimal Control of an Elastic Crane-Trolley-Load System. A Case Study for Optimal Control of Coupled ODE-PDE Systems. *Unpublished.* Preprint, 2017. Submitted to MCMDS.